

Protection Of Water Contaminated By Chemical And Microbial Contaminants For Agriculture: Application Of The Advanced Oxidation Process

H. Bouchaaba^{a*}, R. Maachi^a, N. Nasrallah^a, B. Bellal^b, M. Trari^b, A. Amrane^c

^aLaboratory of Engineering Reaction, Faculty of Mechanic and Engineering Processes USTHB, BP 32, Algiers, Algeria.

^bLaboratory of Storage and Valorization of Renewable Energies, Faculty of Chemistry USTHB, BP 32, Algiers, Algeria.

^c École Nationale Supérieure de Chimie de Rennes, UMR CNRS 6226, 11 allée de Beaulieu, CS 50837, 35708 Rennes Cedex 7.

*Corresponding author: hafida.bouchaaba@gmail.com;

ARTICLE INFO

Article History:

Received : 18/03/2016

Accepted : 20/01/2017

Key Words:

photocatalysis,
ZnO–SnO₂ heterosystem,
alizarin red S,
sunlight irradiation,
Langmuir- Hinshelwood
model.

ABSTRACT/RESUME

Abstract: This paper reports the synthesis, characterization and photocatalytic degradation of alizarin red S (ARS) on the novel new hetero-system ZnO–SnO₂. The hetero-system, prepared by chemical route, was characterized by spectroscopy, energy dispersive spectroscopy (EDS) analysis, microscopy, diffuse reflectance and powder X-ray diffraction. Photo-degradation of ARS was investigated on ZnO, SnO₂ and ZnO– SnO₂ hetero-system. The effect of catalysis dose, initial pH, initial concentration were investigated, the photocatalytic degradation was performed under sunlight irradiation, 84% of (20 mg/L) was degraded within 120 min for concentration. Batch kinetic experiments showed that the degradation follows a pseudo- first-order kinetic with a high correlation coefficient (0.994) according to the Langmuir-Hinshelwood model.

I. Introduction

In recent decades, a growing activity has been observed, regarding to the water pollution by the industrial activities of dyes, pesticides, pharmaceutical compounds and heavy metals [1, 2]. Dye-containing wastewater discharged from the textile industry is a serious threat for the aquatic environment. They affect dramatically the aquatic life and disturb the eco-system for concentration as low as 5 ppm, thus inhibiting the photosynthetic process [3]. To remedy to such that situation, efficient and low cost techniques have been developed to treat the industrial effluents. However, depending on the nature and concentration of the dye, the decontamination method is limited, either because of the expensive cost of operations or inefficiency of the technique to achieve a high degree of purification, respecting the water

standards quality imposed by the World Health Organization (WHO) [4]., The principle is based on the absorption by a semiconductor, of light photons with energy higher than the band gap (E_g). This energy causes the excitation of an electron from the valence band (VB) to the conduction band (CB) and generates a "hole", thus giving the strong photo-redox properties [5, 6]. Algeria has a huge solar potential with an average insolation of 6 kWh m⁻² day⁻¹ and a sunshine duration going over ~ 3000 h/year.

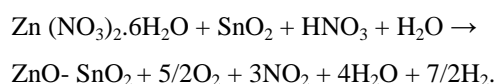
Alizarin red (AR) is a dye soluble in water; it is a pH indicator whose colour changes from yellow to red over the pH range (6.8–8.0) and is widely used in the textile industry and as tracer. AR has the structure as follows: [3]. Many commercial dyes resist to biodegradation and photolysis, so the photocatalysis is highly recommended for their

removal and the (d removal and the advanced oxidation process (AOP) is extensively used [7, 8]. In aqueous solutions, H₂O and O₂ react with the photocarriers (electrons and holes) to form respectively hydroxyl radicals OH[•] and O₂[•] responsible in the oxidation in the organic degradation [9]. This work deals with the synthesis of the semi conducting hetero-system ZnO-SnO₂ and its application for the photo-oxidation of AR under sunlight. We start by a detailed photoelectrochemical (PEC) study to predict the interfacial reactions. Then, the optimization of physical parameters like the initial AR concentration, catalyst dose, agitation speed for the oxidation of AR is undertaken.

II. Materials and methods

II. 1. Catalyst Preparation

ZnO-SnO₂ is prepared by chemical route from Zn(NO₃)₂·6H₂O and SnO₂; stoichiometric amounts are dissolved in a minimum of HNO₃ (69%) and maintained overnight at room temperature. The solution is evaporated on a hot plate and denitrified at 400 °C.



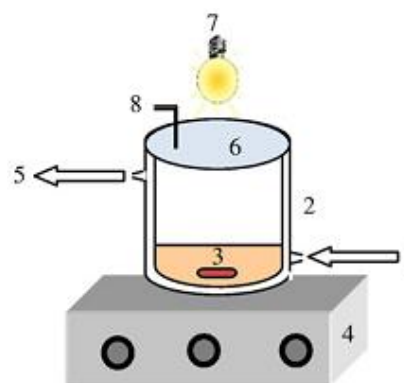
The powder is homogenized in an agate mortar and heated at 850 °C in an alumina crucible with intermediate regrinding. The X-ray diffraction (XRD) is recorded using monochromatized Cu K α radiation. The crystallites size is evaluated from the full width at half maximum using X-powder software and the Williamson Hall plot.

The electrode of ZnO-SnO₂ is prepared by pressing the powder into pellets ($\varnothing = 13$ mm) and sintering at 850 °C, the compactness averages 90%. The back contact is made with a copper wire and silver paint onto the entire area to ensure a uniform current distribution; the pellets are enrobed in glass tube with epoxy resin. The Mott-Schottky plots to evaluate the flat band potential in the working solution are measured in standard cell using a PGZ301 potentiostat; the measurements are done at a frequency of 10 kHz.

II. 2. Photocatalysis Experiments

Alizarin red is selected for the photocatalytic test, the stock solution (1 g L⁻¹) is prepared by dissolving AR in distilled water and diluted to get the concentrations over the range (5-30 ppm). The photocatalytic experiments are done in batch mode using a double walled Pyrex reactor connected to a

thermostated bath (*Figure.1*); the temperature is regulated at 25 °C.



1: Water inlet, 2: Double walled reactor, 3: Stir bar, 4: Magnetic stirrer, 5: Water outlet, 6: Transparent cover, 7: Tungsten lamp, 8: Sampling point.

Figure 1. Schematic of photocatalysis system

The catalyst is maintained in suspension in the solution by magnetic stirring at different speeds. Light is turned on after the adsorption period. The reactor is exposed to sunlight light (109 mW cm⁻²); a variable mass of ZnO-SnO₂ powder (25-125 mg) is dispersed in 100 mL of AR solution. Aliquots are withdrawn at regular time periods during the course of the reaction. The solutions are separated from the catalyst by centrifugation and the residual AR concentration is analyzed with a UV-Vis spectrophotometer (Shimadzu 1800, λ_{max} : 546 nm) According to the Beer's law, the absorbance of the is proportional to the AR concentration. The removal percentage (R %) is calculated from the relation:

$$R(\%)_t = \left[\frac{C_0 - C_t}{C_0} \right] \times 100 \quad (1)$$

Where C_0 is the initial AR concentration (mg/L) and C_t the equilibrium concentration.

III. Results and discussion

III. 1. Catalyst characterization

The XRD pattern of ZnO-SnO₂ prepared by nitrate route (*Figure.2*) is characteristic of mixed phase according to the JCPDS (ZnO: 00- 036.1451, SnO₂: 00-041.1445) [10, 11].

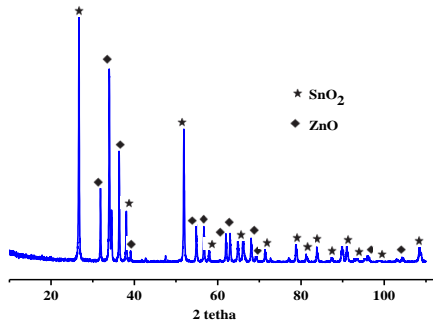


Figure 2. The XRD pattern of ZnO-SnO₂ prepared by nitrate route.

The optical properties bring insights on the energy diagram, a preamble for the photocatalysis. The dependence of the optical absorption coefficient (α) on the energy photon ($h\nu$) is given by the Tauc relation:

$$(\alpha h\nu)^n = C \times (h\nu - E_g) \quad (2)$$

C being a constant and α the optical coefficient, the plot of $(\alpha h\nu)^2$ versus the photon energy ($h\nu$) allows us to determine the optical gap from the intercept of the fitted line to $h\nu = 0$. (Figure. 3) shows a direct gap at 3.14 eV.

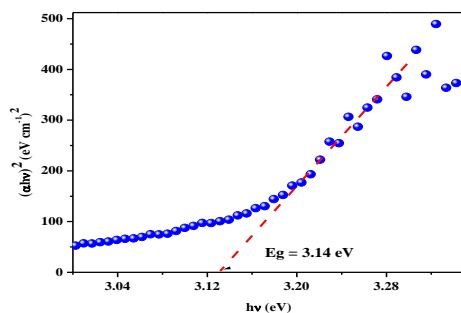


Figure 3. The direct optical transition of the ZnO-SnO₂.

The knowledge of the electronic bands is crucial in photocatalysis, they are determined from the flat band potential (E_{fb}) using the interfacial capacitance (C_{SC}):

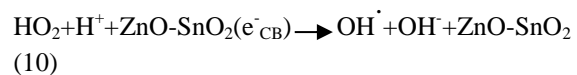
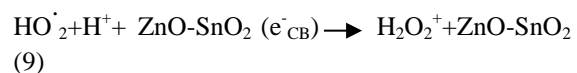
$$C_{SC}^{-2} = \pm 2/\epsilon\epsilon_0 N_D \{E - E_{fb}\} \quad (3)$$

Where ϵ and ϵ_0 are respectively the dielectric constants of the material and vacuum, we have

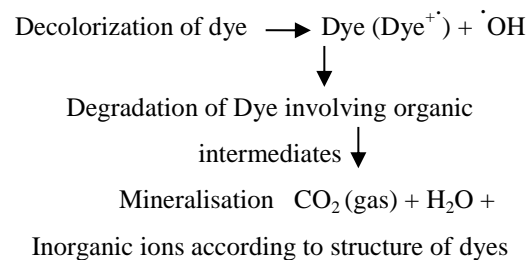
drawn the energy band diagram of the junction ZnO-SnO₂/solution in order to understand how the light mineralizes in aqueous medium.

III.2. Mechanism of AR degradation

ZnO-SnO₂ oxydizes in two ways, photogenerated holes h^+ in the valence band and the OH radicals, which are strongly active and degrading non-selective agents. Valence band holes (h^+ VB) and conduction band electrons (e^- CB) are generated when aqueous ZnO-SnO₂ suspension was irradiated with UV light. These electron-hole pairs interact separately with the substrate. Valence band holes (h^+ VB) react with surface bound H₂O or OH⁻ to produce hydroxyl radical (OH[•]). Valence band holes can also oxidize organic molecule. Conduction band electrons (e^- CB) reduce molecular oxygen to generate superoxide radicals as shown in Eqs. (4) (7). [12].



The mechanism of semiconductor photocatalysis is of very complex nature. Dye molecules interact with O₂^{•-}, OH₂[•] or OH[•] species to generate intermediates ultimately lead to the formation of degradation products. Hydroxyl radical (OH[•]) being very strong oxidizing agent (standard oxidation potential 2.8 eV) mineralizes dye to end product (see Scheme 1) [13, 14].



III. 3. Study of photoactivity of ZnO-SnO₂

The photocatalysis is a clean technology and continues to attract great attention in the water decontamination by hazardous dyes [15- 19]. The solar energy contains ~ 5% of UV light i.e. 60 W of pure ultraviolet and exploring the solar energy for the environmental pollution is an attractive challenge for the advanced oxidation process (AOP) onto ZnO-SnO₂[20, 21], it fills the photocatalytic requirements for the environmental protection since it is non toxic and chemically stable over a wide pH range. The hetero-system is not involved in any redox reaction except as photoconductor to generate electron/hole (e⁻/h⁺) pairs. In addition, it is responsive to UV light and the further advantage resides in the high energy of the conduction band, able to mineralize the organic matter through radicals (Figure. 4). At the working pH (~9); the hetero-system ZnO-SnO₂ is protonated and attract the AR molecules by electrostatic forces, thus facilitating the AOP process.

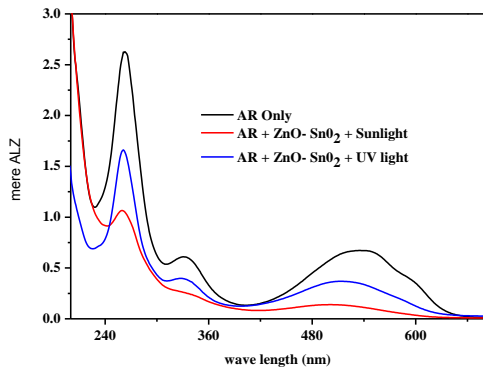


Figure 4. The influence of the light intensity on the ARS photodegradation (ARS= 20 mg/L, pH= 9, T =25 °C and catalyst dose = 0.5g/L).

III. 4. Effect of the dose of ZnO-SnO₂

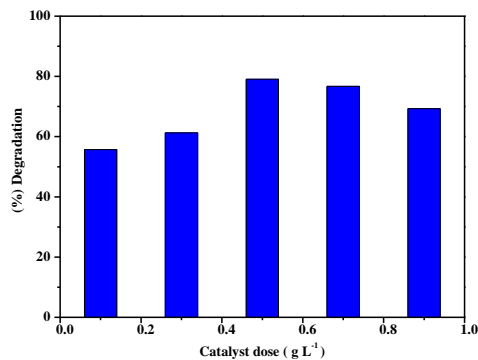


Figure 5. Histogram showing the influence of ZnO- SnO₂ dose on the photoactivity: (C_o: 20 mg/L, temperature: 298 K, reaction time: 180 min, pH ~ 9 and stirring speed: 250 rpm).

At first, the influence of the catalyst dose on the oxidation of AR is investigated under artificial light. Figure. 5 does not show a significant variation of the photoactivity with however an optimal dose (mass of ZnO-SnO₂ /volume of the solution) of 0.5 g L⁻¹. This is simply due to the increasing number of photocatalytic sites, leading to a higher reception surface for incident photons and in this way an increasing number of generated electron/hole (e⁻/h⁺) pairs.

III. 5. Effect of agitation rate

The effect of stirring speed of the powder suspension on the photoactivity is also investigated. A maximal adsorption capacity is obtained for a speed of 250 rpm (Figure. 6); such moderate value gives the best homogeneity for the catalyst suspension. At high speeds, the vortex phenomenon occurs with an inclination angle of the solution; the suspension is no longer homogeneous, making the AR degradation difficult. By contrast, at low speeds, the surface is nearly horizontal and receives more photons while the powder is at the bottom of the reactor.

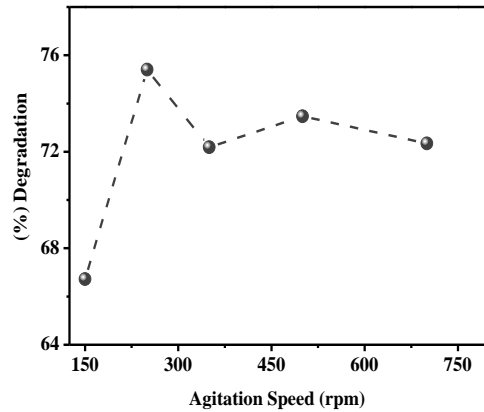


Figure 6. Effect of the stirring speed on the photodegradation (C_o: 20 mg/L; catalyst dose: 0.5 g/L; pH~9)

III. 6. Photodegradation kinetic of AR

The photoactivity occurs in different stages: bulk and film diffusion are generally rapid and are not rate determining. The pseudo first order and second order are applied to fit the experimental data and to elucidate the photo-oxidation kinetic. To determine the order of the reaction, we plotted the reciprocal concentration (C⁻¹) versus time (Figure. 7) obtaining two lines indicates an apparent kinetics of AR oxidation. The results are summarized in Table 1. The oxidation rate depends on the initial concentration (C_o) and the process is well described by a pseudo- first order r kinetic [22]:

$$r = k_{app}[C]^2 = -\frac{dC}{dt} \quad (12)$$

The integration form gives:

$$\int_{C_0}^C -\frac{dC}{C^2} = \int_0^t k_{app} dt \quad (13)$$

a/ Pseudo first order

$$\ln \left[\frac{C_0}{C} \right] = K_{app} t \quad (14)$$

b/ Pseudo second order

$$\frac{1}{C} = \frac{1}{C_0} + K_{app} t \quad (15)$$

Our desire is to extend the experiments under direct solar irradiation. The tests are performed on the roof of our Laboratory (latitude 36.8°North, longitude 3.1°West). The solar flux(108.5 mW cm²) is measured with a digital light meter (roline RO 1332).

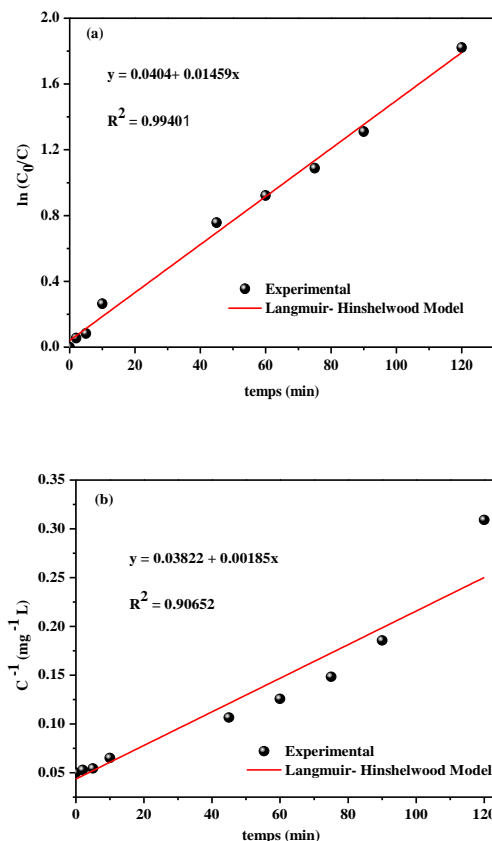


Figure 7. The modeling of ARS photodegradation with the Langmuir–Hinshelwood model (a): pseudo first order and (b): pseudo second order (catalyst dose: 0.5 g/L, sunlight).

k_{app} (L mg⁻¹ mn⁻¹) is the apparent rate constant. The plots of $\ln(C)$ and C^{-1} versus the time (t). The constants k_{app} and the correlation coefficients (R^2) are gathered in Table 1, k_{app} decreases with increasing C_0 and the photo-degradation kinetic obeys to the Hinshelwood-Langmuir model [23].

Tableau. 1. Kinetic Parameters of the first and pseudo-second-order model of AR onto ZnO– SnO₂ hetero-system under sunlight irradiation.

C ₀ (mg/L)	Pseudo first-order		Pseudo-second-order	
	K ₁ (min ⁻¹)	R ²	K ₂ (L mg ⁻¹ min ⁻¹)	R ²
20	0.01459	0.99401	0.00185	0.90652

The initial concentration (20 ppm) kept overnight in the dark in presence of ZnO-SnO₂, decreases by 10% due to the adsorption. Then the reactor is exposed to sunlight, a complete and rapid degradation occurs in less than 180 min (Figure. 7). Such improvement is mainly due to the stronger absorption of both catalysts under solar light which contains about 60 W of ultraviolet radiation.

In a region with a high solar potential like Algeria (~ 6kWh/m²/day), the exploitation of solar radiation for the treatment of chemical and microbial contaminants is highly desirable.

IV. Conclusion

This work aimed the study of the elimination of a synthetic dye namely the alizarin red S present in the textile and industries, by heterogeneous photocatalysis on the novel ZnO-SnO₂ synthesized by chemical route in order to increase the active surface area, was characterized by various physical methods (XRD, diffuse reflectance). The X-ray diffraction confirms the mixed phases in order to confirm the purity of this catalyst as well as knowing their physical and optical Properties

The application of this hetero-system in the treatment of alizarin red S as model effluent by photocatalysis in solar light was successful and proved its stability, reliability and efficacies in the elimination of chemical pollutants found in wastewater.

V. References

1. E. Brillas, C-A. Martínez-Huitle: Decontamination of wastewaters containing synthetic organic dyes by

- electrochemical methods. *Applied Catalysis B: Environmental*, 604, 166–167 (2015).
2. C-A. Martínez-Huitle, E. Brillas: Decontamination of wastewaters containing synthetic organic dyes by electrochemical methods: A general review, *Applied Catalysis B: Environmental*, 106, 3–4 (2009).
 3. M- A. Rauf, M- A. Meetani, S. Hisaindee: An overview on the photocatalytic degradation of azo dyes in the presence of TiO₂ doped with selective transition metals, *Desalination*, 14, 1–3 (2011).
 4. J- L. Domingo, M. Nadal: Carcinogenicity of consumption of red and processed meat: What about environmental contaminants, *Environmental Research*, 110, 145 (2016).
 5. S- Kumar, Kansal, R. Lamba, S- K. Mehta, A. Umar: Photocatalytic degradation of Alizarin Red S using simply synthesized ZnO nanoparticles, *Materials Letters*, 386 106 (2013).
 6. R. Satheesh, K. Vignesh, A. Suganthi, M. Rajaraja: Visible light responsive photocatalytic applications of transition metal (M = Cu, Ni and Co) doped α -Fe₂O₃ nanoparticles, *J Environmental Chemical Engineering*, 1957, 2(2014).
 7. D-A.Vallero : Contaminant Hazards Environmental Contaminants, 435-497, *Chapter 9* (2004).
 8. B- W. David, M- S. Christie: Routes of Exposure to Nanoparticles: Hazard Tests Related to Portal Entries, *Nanoengineering, Chapter 1.2*, 42-54 (2015).
 9. A. Tsaboula, E- N. Papadakis, Z. Vryzas, A. Kotopoulou, K. Kintzikoglou, E. Papadopoulou-Mourkidou: *Environmental and human risk hierarchy of pesticides: A prioritization method, based on monitoring, hazard assessment and environmental fate*, *Environment International*, 78-93, 91(2016).
 10. J. Haider, M- S- J. Hashm: 8.02 - Health and Environmental Impacts in Metal Machining Processes, *Reference Module in Materials Science and Materials Engineering, from Comprehensive Materials Processing*, 7-33, 8, (2014).
 11. H- F. Hemond, E- J. Fechner: Surface Waters Chemical Fate and Transport in the Environment (Third Edition), 75-218, *Chapter 2*(2015).
 12. Liqun. Ye, Kejian. Deng, Xu. Feng, Lihong Tian, Tianyou. Peng, Ling. Zan, Increasing visible-light absorption for photocatalysis with black, *Phys. Chem.* 14 (2012) 82–85.
 13. W.F. Jardim, S.G. Moraes, M.M.K. Takiyama, Photocatalytic degradation of aromatic chlorinated compounds using TiO₂: *toxicity of intermediates*, *Water Res.* 31 (1997) 1728–1732.
 14. K. Vinodgopal, I. Bedja, S. Hotchandani, P.V. Kamat, A photocatalytic approach for the reductive decolorization of textile azo dyes in colloidal semiconductor suspensions, *Langmuir* 10 (1994) 1767–1771.
 15. H. Bouchaaba, B. Bellal, R. Maachi, M. Trari, N. Nasrallah, A. Mellah : Optimization of physico-chemical parameters for the photo-oxidation of neutral red on the spinel Co₂SnO₄, *J of the Taiwan Institute of Chemical Engineers*, 1–8, 000 (2015).
 16. B. Sørensen: The Energy Conversion Processes, *Renewable Energy (Fourth Edition)*, 337-531, *Chapter 4*(2011).
 17. H. Mekatel, S. Amokrane, B. Bellal, M. Trari, D. Nibou: Photocatalytic reduction of Cr(VI) on nanosized Fe₂O₃ supported on natural Algerian clay: Characteristics, kinetic and thermodynamic study, *Chemical Engineering Journal*, 611–618, 200–202 (2012). *Journal of Hazardous Materials* 153 (2008) 1222-1234.
 18. S. Giannakis, M. Voumard, D. Grandjean, A. Magnet, L- F- D. Alencastro, C. Pulgarin : Micropollutant degradation, bacterial inactivation and regrowth risk in wastewater effluents: Influence of the secondary (pre)treatment on the efficiency of Advanced Oxidation Processes, *Water Research*, 505-515, 102(2016).
 19. S. Cataldo, A. Ianni, V. Loddo, E. Mirenda, L. Palmisano, F. Parrino, D. Piazzese: Combination of advanced oxidation processes and active carbons adsorption for the treatment of simulated saline wastewater, *Separation and Purification Technology*, 101-111, 171(2016).
 20. M. Brienza, M- M. Ahmed, A. Escande, G. Plantard, L. Scrano, S. Chiron, S- A. Bufo, V. Goetz: Use of solar advanced oxidation processes for wastewater treatment: Follow-up on degradation products, acute toxicity, genotoxicity and estrogenicity, *Chemosphere*, 473-480, 148(2016).
 21. S- O. Ganiyu, E- D. Van Hullebusch, M. Cretin, G. Esposito, M- A. Oturan: Coupling of membranefiltrationand advanced oxidation processes f or removal of pharmaceutical residues: A critical review *Original Research Article Separation and Purification Technology*, 891-914, 156 (2015).
 22. J- R. Alvarez-Corena, J- A. Bergendahl, F- L. Hart: Advanced oxidation of five contaminants in water by UV/TiO₂: Reaction kinetics and byproducts identification, *J Environmental Management*, 544-551, 181(2016).
 23. H. Sudrajat, S. Babel: A new, cost-effective solar photoactive system N-ZnO-polyester fabric for degradation of recalcitrant compound in a continuous flow reactor, *Materials Research Bulletin*, 369-378, 83(2016).

Please cite this Article as:

Bouchaaba H., Maachi R., Nasrallah N., Bellal B., Trari M., Amrane A., *Biosorption of Nickel(II) ions from aqueous solutions by using Chicken eggshells as low-cost biosorbent, Algerian J. Env. Sc. Technology*, 3:1 (2017) 09-14